



1 **Measurement report: Long-term measurements of aerosol precursor concentrations in the Finnish sub-**
2 **Arctic boreal forest**

3 Tuija Jokinen^{1,2*}, Katrianne Lehtipalo^{1,3}, Roseline Cutting Thakur¹, Ilona Ylivinkka¹, Kimmo Neitola¹, Nina
4 Sarnela¹, Totti Laitinen¹, Markku Kulmala¹, Tuukka Petäjä¹ and Mikko Sipilä¹

5 ¹Institute for Atmospheric and Earth System Research (INAR) / Physics, Faculty of Science, University of
6 Helsinki, P.O. Box 64, Helsinki, 00014 University of Helsinki

7 ²Climate & Atmosphere Research Centre (CARE-C), The Cyprus Institute, P.O. Box 27456, Nicosia, CY-
8 1645, Cyprus

9 ³Finnish Meteorological Institute, Helsinki, Finland

10 *correspondence to t.jokinen@cyi.ac.cy

11

12 **Abstract:**

13 Aerosol particles form in the atmosphere by clustering of certain atmospheric vapors. After growing to larger
14 particles by condensation of low volatile gases, they can affect the Earth's climate directly by scattering light
15 and indirectly by acting as cloud condensation nuclei. Observations of low-volatility aerosol precursor gases
16 have been reported around the world but longer-term measurement series and any Arctic data sets showing
17 seasonal variation are close to non-existent. In here, we present ~7 months of aerosol precursor gas
18 measurements performed with the nitrate based chemical ionization mass spectrometer (CI-API-TOF). We
19 deployed our measurements ~150 km North of the Arctic Circle at the continental Finnish sub-Arctic field
20 station, SMEAR I, located in Värriö strict nature reserve. We report concentration measurements of the most
21 common new particle formation related compounds; sulfuric acid (SA), methane sulfonic acid (MSA), iodic
22 acid (IA) and a total concentration of highly oxygenated organic compounds (HOMs). At this remote
23 measurement site, SA is originated both from anthropogenic and biological sources and has a clear diurnal
24 cycle but no significant seasonal variation. MSA shows a more distinct seasonal cycle with concentrations
25 peaking in the summer. Of the measured compounds, iodic acid concentrations are the most stable throughout
26 the measurement period, except in April, when the concentration of IA is significantly higher than during the
27 rest of the year. Otherwise, IA has almost identical daily maximum concentrations in spring, summer and
28 autumn, and on new particle formation event or non-event days. HOMs are abundant during the summer
29 months and low in winter months. Due to the low winter concentrations and their high correlation with ambient
30 air temperature, we suggest that most of HOMs are products of biogenic emissions, most probably
31 monoterpene oxidation products. New particle formation events at SMEAR I happen under relatively low
32 temperatures with a fast temperature rise in the morning followed by decreasing relative humidity during the
33 day. The ozone concentrations are on average ~10 ppbv higher on NPF days than non-event days. During NPF
34 days, we have on average higher SA concentration peaking at noon, higher MSA concentrations in the
35 afternoon and slightly higher IA concentration than during non-event days. All together, these are the first long
36 term measurements of aerosol forming vapors from the SMEAR I in the sub-arctic region, and the results help
37 us to understand atmospheric chemical processes and aerosol formation in the rapidly changing Arctic.

38 **Introduction:**

39 The climate of sub-Arctic region is characterized with some of the most extreme temperature variations on
40 Earth. We expect that during the course of the 21st century, the boreal forest is to experience the largest increase
41 in temperatures of all forest biomes (IPCC, 2013), making it the most vulnerable to climate change. The boreal
42 forest (taiga) covers most of the sub-Arctic and encompasses more than 30% of all forests on Earth, being one
43 of the largest biome in the world (Brandt et al., 2013). The expected rate of changes, may overwhelm the
44 resilience of forest ecosystems and possibly lead to significant biome-level changes (Reyer et al., 2015). The
45 forest-atmosphere systems are closely interlinked to one another. The forest stores carbon and water in the



46 peat, soil and as biomass while at the same time vegetation emits volatile organic compounds (VOC) into the
47 atmosphere (Bradshaw and Warkentin, 2015). In the Arctic, summer is short, but solar radiation is abundant
48 and extends the daylight hours all the way to midnight and beyond. On the other hand, during the polar night
49 air pollutants accumulate in the atmosphere due to cold and stable atmosphere, while turbulent mixing is
50 inhibited, and the lack of removal processes lead to the formation of Arctic haze (Stohl, 2006). These features
51 make the Arctic an interesting study region for photochemistry of reduced atmospheric compounds. Oxidation
52 processes that dominantly occur in the summer time control the processes removing VOCs and other traces
53 gases, such as SO₂ and NO_x, from the atmosphere in the Arctic. Detailed understanding of atmospheric
54 processes leading to aerosol precursor formation and gas-to-particle conversion and their role in feedback
55 mechanisms help in assessing the future climate.

56 Aerosol and trace gas measurements in the sub-Arctic field station SMEAR I, go back to the 90s (Ahonen et
57 al., 1997; Kulmala et al., 1998; Mäkelä et al., 1997). Trace gas and aerosol measurements at SMEAR I started
58 in 1992 making them one of the longest continuous measurements of aerosol particle number and size
59 distributions in the Arctic (Ruuskanen et al., 2003). These long-term measurements show that aerosol particles
60 regularly form and grow from very small sizes (< 8 nm diameter) with the highest frequency in the spring,
61 between March and May (Dal Maso et al., 2007; Vehkamäki et al., 2004). It is suggested, that spring promotes
62 new particle formation (NPF) because of the awakening of biological processes after the winter. At SMEAR I
63 the snow only melts away in May-June and thus, many biological processes (photosynthesis) activate while
64 the snow is still deep. This makes the Arctic spring a very complex environment for atmospheric chemistry
65 with possible emission sources from melting snow, ice, melt water, vegetation and transport from other areas.
66 At SMEAR I, most of the observed NPF events are either connected to clean air arriving from the Northern
67 sector (originating from The Arctic Ocean and transported over boreal forest, Dal Maso et al., 2007) or the
68 polluted air masses from the Eastern sector (Kyrö et al., 2014; Sipilä et al., 2021). Annually, around 30-60
69 NPF events are recorded at SMEAR I, of which around half could be initiated by anthropogenic air pollutants
70 from the Kola Peninsula (Kyrö et al., 2014; Pirjola et al., 1998; Sipilä et al., 2021) leaving half of the events
71 occurring from natural sources. The trend of NPF occurrence in Värriö is decreasing, as the anthropogenic
72 sulfur dioxide emissions are decreasing in Russia (Kyrö et al., 2014).

73 Formation and growth of new particles at SMEAR I usually happen during daylight, highlighting the
74 importance of photochemical activities. However, unlike most other locations, NPF is also observed during
75 nighttime or polar night (Kyrö et al., 2014; Vehkamäki et al., 2004). Formation and growth processes of
76 aerosols seem not to be correlated with each other at SMEAR I (Vehkamäki et al., 2004). Earlier literature
77 reports, that the formation rate (J) has no clear seasonal trend, while the growth rates (GR) of small particles
78 clearly peak during summer (Ruuskanen et al., 2007). This indicates that different chemistry drives the initial
79 cluster formation and the subsequent growth processes. From the observed nucleation rates it has been
80 proposed that NPF at SMEAR I could be due to sulfuric acid –ammonia (-water) nucleation (Napari et al.,
81 2002) likely dominated by ion-induced channel at least during winter months (Sipilä et al., 2021). Kyrö et al.,
82 2014 concludes that 20-50% of the condensational growth can also be explained by sulfuric acid in Värriö.
83 Other studies speculate about the possibility of different organic compounds participating in NPF in the sub-
84 Arctic. Tunved et al., 2006 studied the air masses arriving to SMEAR I station and concluded that the aerosol
85 mass increased linearly with time that the air masses travelled over land. The concentration of condensing
86 gases over the boreal forest was concluded to be high and most likely consisting mainly of oxidation products
87 of terpenes (VOCs) that are emitted by the forest. At SMEAR II station in Hyytiälä, approximately 700 km
88 South-West of Värriö, oxidized organics mostly explain the growth of newly formed particles (Bianchi et al.,
89 2017; Ehn et al., 2014). However, direct measurements of the aerosol forming and growing vapor species are
90 still lacking from SMEAR I except during wintertime without biogenic activity when sulfuric acid has been
91 shown to be primarily responsible on formation and growth (Sipilä et al., 2021). In Värriö, the role of NPF is
92 critical in forming of cloud condensation nuclei (CCN), since measurements show that the number of CCN
93 can increase up to 800 % as a result of NPF (Kerminen et al., 2012). In other locations in the boreal forest and
94 Arctic, some measurements shed light into the possible chemical components that could be forming particles
95 in Värriö. Currently, the closest continuous measurements with the nitrate based CI-API-TOF are conducted



96 in Hyytiälä at the SMEAR II-station (Jokinen et al., 2012, 2017; Kulmala et al., 2013). In Hyytiälä there is
97 direct evidence on the key role of the photochemical production of sulfuric acid and HOMs maintaining
98 atmospheric NPF (Bianchi et al., 2017; Ehn et al., 2014; Jokinen et al., 2017; Kulmala et al., 2013).

99 Other chemical composition measurements of aerosol precursors have been conducted only in a few locations
100 in the High-Arctic and over the Arctic Ocean (Baccarini et al., 2020; Beck et al., 2021; He et al., 2021; Sipilä
101 et al., 2016). These studies show that in the Arctic, the marginal ice zone and the coast of the Arctic Ocean is
102 a source of atmospheric iodic acid that is efficiently forming new particles. Sulfuric acid and MSA
103 concentrations were also reported (Beck et al., 2021), but they were much lower in concentration than iodic
104 acid (Baccarini et al., 2020). However, the chemistry behind NPF is not that simple, even the pristine Arctic
105 air. The clean air above the Arctic Ocean is abundant in dimethyl sulfide (DMS) emitted by phytoplankton,
106 that rapidly oxidizes into sulfuric acid and MSA on sunny days and consequently forms cloud condensation
107 nuclei (Charlson et al., 1987; Park et al., 2018). Beck et al., (2021) report, that in Svalbard in the Arctic Ocean,
108 sulfuric acid and methane sulfonic acid contribute to the formation of secondary aerosol. They also observed
109 that these compounds formed particles large enough to contribute to some extent to cloud condensation nuclei
110 (CCN). This is supported by measurements of aerosol chemical composition from the Arctic that commonly
111 report MSA in particulate matter (Dall'Osto et al., 2018; Kerminen et al., 1997). According to Beck et al.
112 (2021) the initial aerosol formation in the high Arctic occurs via ion-induced nucleation of sulfuric acid and
113 ammonia and subsequent growth by mainly sulfuric acid and MSA condensation during springtime and highly
114 oxygenated organic molecules (HOM) during summertime. By contrast, in an ice-covered region around
115 Villum, Greenland, Beck et al. (2021) observed new particle formation driven by iodic acid, but the particles
116 remained small and did not grow to CCN sizes due to insufficient concentration of condensing vapors. Since
117 the Arctic CCN number concentrations are low in general, formation of new particles is a very sensitive process
118 affecting the composition of the aerosol population and CCN numbers in the area. Also in Värriö, the role of
119 NPF is critical in forming of cloud condensation nuclei (CCN), since measurements show that the number of
120 CCN can increase up to 800 % as a result of NPF (Kerminen et al., 2012).

121 In this article, we present the measurements of aerosol precursor molecules from the continental SMEAR I
122 station, ~150 km North of the Arctic Circle and ~150 km from the Arctic Ocean. We measured sulfuric acid,
123 methane sulfonic acid, iodic acid and highly oxygenated organic compound concentrations with a sulfuric acid
124 calibrated CI-APi-TOF (Jokinen et al., 2012; Kürten et al., 2012) to determine their levels in the sub-Arctic
125 boreal forest and to understand whether these species are connected with the aerosol formation process in the
126 area.

127 **Methods, measurement site and instrumentation:**

128 The core of this work is measurements of gas phase aerosol precursors. We use the nitrate chemical ionization
129 atmospheric pressure interface time-of-flight mass spectrometer (CI-APi-ToF) that has been operational at the
130 SMEAR I-station (N67°46, E29°36) in Eastern-Lapland since the early spring of 2019. SMEAR stands for
131 Station for Measuring Ecosystem – Atmosphere Relations. Measurements were done on top of Kotovaara hill
132 (390 m a.s.l.), close to ground level in an air-conditioned small log wood cottage. The cottage is surrounded
133 by ~65-year-old Scotts pine forest. More details about the station can be found in earlier publications (Hari et
134 al., 1994; Kyrö et al., 2014). The mass spectrometric measurements are designed to start a long-term
135 measurement series of atmospheric aerosol forming trace gases in the Finnish Lapland and the measurements
136 are ongoing to this day. We measure e.g. sulfuric acid, iodic acid, highly oxygenated organic molecules and
137 methane sulfonic acid with high time resolution and precision. The measurements are running in Finnish winter
138 time (UTC+2) throughout the year.

139 We calibrated the CI-APi-TOF twice during the measurement period and run the instrument with the same
140 settings for the whole measurement period reported in this paper. We calibrated the instrument using a sulfuric
141 acid calibrator described in Kürten et al., 2012. The calibration factor from the two separate calibrations were
142 1) $7 \cdot 10^9$ and 2) $8 \cdot 10^9$ and we use the average $7.5 \cdot 10^9$ in our study calculate the concentrations of all reported
143 compounds. This factor includes the loss parameter due to the ~1 m long unheated inlet tube (3/4" stainless



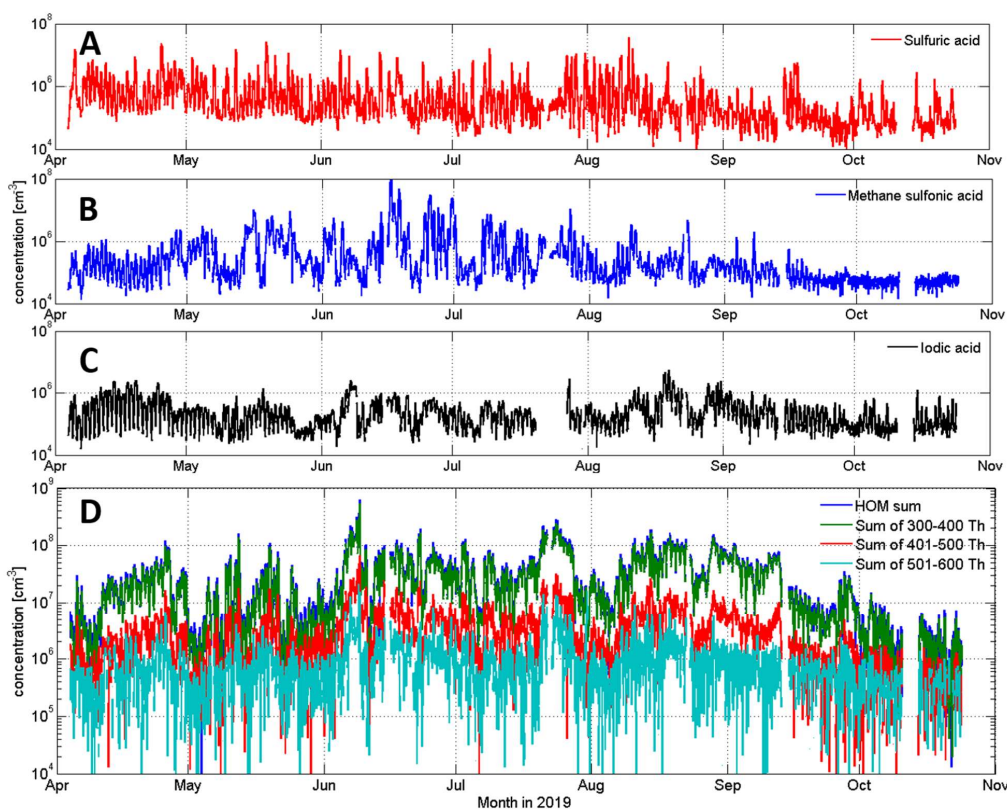
144 steel). HOMs and iodic acid have been estimated to be charged similarly at the kinetic limit as sulfuric acid
145 (Ehn et al., 2014; Sipilä et al., 2016), so the calibration factor for them should be similar, but please note, that
146 the concentration of other compounds than SA can be highly uncertain due to different ionizing efficiencies,
147 sensitivities and other unknown uncertainties. The sulfuric acid, iodic acid and MSA data presented in this
148 study are all results of high-resolution peak fitting of the CI-API-TOF, in order to avoid inaccurate
149 identification of compounds and to separate overlapping peaks. The HOM data is a sum of mass-to-charge
150 ratios from 300 to 400 Th, representing the monomer HOM range (C_{10} compound range), 401 to 500 Th for
151 the slightly larger HOMs (C_{15} compound range) and 501 to 600 Th for the dimer species (C_{20} compound range).
152 We also give the sum of these all (from 300 to 600 Th). The goal of this article is not to specify different HOM
153 compounds or to study NPF in mechanistic details but to give an overview of general seasonal trends and
154 variations of these selected species. Note that since this is a sum of all peaks in the selected mass range, we
155 cannot assure that all the compounds included are HOMs. However, the investigation in laboratory conditions
156 show that the nitrate-CI-API-TOF is highly selective and sensitive towards HOMs with $O > 5$ (Riva et al.,
157 2019) and with hydroperoxide (-OOH) functionalities (Hytinen et al., 2015). All data obtained from the CI-
158 API-TOF we analyzed using tofTools program described in (Junninen et al., 2010) and averaged over an hour.
159 The original data time resolution is 5 sec. The uncertainty range of the measured concentrations reported in
160 this study is estimated to be $-50\%/+100\%$ and the limit of detection, LOD $4 \cdot 10^4$ molecules cm^{-3} (Jokinen et
161 al., 2012).

162 To classify NPF events recorded during the measurement period, we used the data measured by a Differential
163 Mobility Particle Sizer (DMPS). The DMPS instrument and earlier statistics of NPF events in Värriö has been
164 documented by (Dal Maso et al., 2007; Vana et al., 2016; Vehkamäki et al., 2004). The NPF events were
165 classified according to (Dal Maso et al., 2005). Total aerosol particle number concentration was measured with
166 a Condensation Particle Counter (CPC, TSI 3776) in the size range of 3 – 800 nm. Air ion size distributions
167 were measured with the Neutral cluster and Air Ion Spectrometer, NAIS (Kulmala et al., 2007; Manninen et
168 al., 2016; Mirme and Mirme, 2013) that measures negative and positive ions in the size range of 0.8 – 42 nm
169 in mobility diameter and total particle size distribution between ~ 2 and 42 nm. All meteorological parameters,
170 trace gas concentrations and aerosol data we downloaded directly from smartSMEAR open access database
171 (<https://smear.avaa.csc.fi/>) and all mass spectrometric data are available on request.

172 **Results and discussion:**

173 **a. Overview of the whole measurement period:**

174 You can see a time series of the most common aerosol precursor compounds; sulfuric acid, methane sulfonic
175 acid, iodic acid and sums of different HOM groups in Figure 1. This figure depicts the whole measurement
176 period from April 4 to October 27 in 2019. Overall, we succeeded to measure the whole 7 month period almost
177 uninterruptedly. Only a few short power cuts stopped our measurements during this time. Iodic acid data is
178 missing from late July since its peak could not be separated well enough from overlapping peaks in the spectra
179 during this time. This was due to poor resolution (low signal of IO_3^- close to another peak) that makes peak
180 integration to give negative, unreal values and we thus decided to flag them out. After late October, the
181 instrument malfunctioned and stopped our measurements. In this particular article, we present data from spring
182 (Apr-May), summer (Jun-Jul-Aug) and autumn (Sep-Oct) 2019. More about the SMEAR I winter observations
183 can be read in Sipilä et al., 2021 where they report observations of polar night pollution events from Värriö after
184 the CI-API-TOF was fixed.



185

186 **Figure 1.** Overview of sulfuric (A), methane sulfonic (B) and iodine (C), as well as HOM (D)
187 concentrations at SMEAR I in April to October 2019. All data in panels A-C are resulting from high-resolution
188 peak fitting. HOM data are sums of certain mass ranges; from 300 to 400 Th in green, representing C10 or
189 HOM monomer compounds, from 401 to 500 Th in red, representing C15 compound and from 501 to 600 Th
190 on light blue, representing C20 or HOM dimer compounds. The sum of HOM (blue) is a sum of the
191 aforementioned mass ranges. The sum of HOMs is approximately one order of magnitude higher than SA,
192 MSA or IA concentrations during this measurement period.

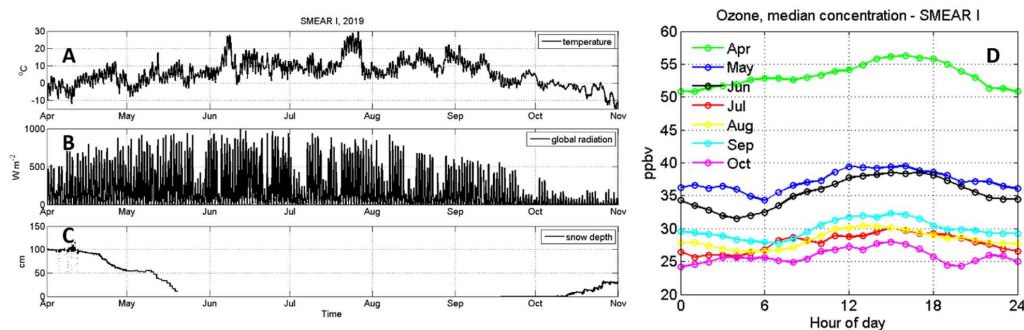
193 In Figure 2 we show some of the most interesting environmental and meteorological parameters that influence
194 the atmospheric gas composition during the measurements period; temperature, global radiation and snow
195 depth (Figure 2A). There are some special features in year 2019; the summer had two heat waves, when the
196 air temperature rose up to 29.2 °C in early June and to almost the same values in late July. These episodes are
197 getting more common in Lapland due to climate change. These warmer conditions will probably change the
198 emissions of trace gases including the composition and abundance of aerosol precursors in the future Arctic
199 environment (Schmale et al., 2021).

200 From Figure 2, we see that the snow covered period ended in 2019 in late May and snow started to accumulate
201 again in mid-October. Solar radiation (Figure 2A) is intense in Värriö during springtime and gives Värriö
202 favorable photo-oxidizing conditions, effectively removing air pollutants and trace gases from the atmosphere.
203 Photochemical activity produces ozone in springtime and this is visible in very high ozone concentrations at
204 the site (Figure 2B). Ozone concentrations were around 55 ppbv in April and decreased to ~30 ppbv in the late
205 summer and autumn (Figure 2B). The spring ozone concentration in 2019 was significantly higher than the



206 previous reports from the years 1992 to 2001, when monthly mean concentrations of ozone varied between
207 25-40 ppbv (Ruuskanen et al., 2003).

208



209

210 **Figure 2:** Observations of temperature (A), global radiation (B) and snow depth (C) at SMEAR I during the
211 measurement period. Monthly median ozone concentration in ppbv (D), is showing the relatively high level of
212 ground level ozone during springtime (Apr).

213 The springtime diurnal solar cycle is clearly visible with all studied compounds. All measured aerosol
214 precursor compounds are abundant even during the period when snow covers the ground in the spring. The
215 HOM concentrations follow the increasing solar radiation and rising temperature. MSA has a stronger diurnal
216 cycle before the snow melt than after it. This may be due to rain and cloudy conditions that are more common
217 in the summer. Sulfuric acid and iodic acid do not have such strong seasonal variation than HOMs and MSA.
218 The aerosol precursor concentrations are discussed in more detail in the following sections.

219 Seasonal and monthly variation of SA, MSA, iodic acid and HOM concentrations

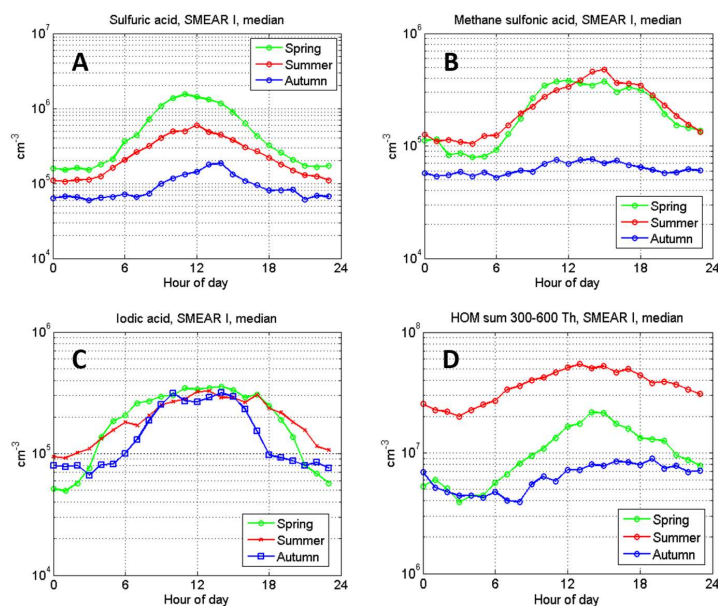
220 We present the diurnal variation of aerosol precursors; sulfuric acid, methane sulfonic acid, iodic acid and
221 highly oxygenated molecule, concentrations separately for different seasons in Figure 3. Strong seasonality is
222 most evident in sulfuric acid and HOM concentrations. SA is at its highest in the spring, decreasing toward
223 summer and autumn while HOMs reach their maximum in the summer. The increase in HOMs in the summer
224 at SMEAR I is linked to the increased emissions of VOCs from vegetation that oxidize into HOMs via
225 ozonolysis (Ehn et al., 2014) and OH-radical reactions (Berndt et al., 2016; Jokinen et al., 2014, 2017; Wang
226 et al., 2018). The overall lowest aerosol precursor concentrations we detect during autumn (winter data was
227 missing from this study, see Sipilä et al. 2021, for winter time observations made promptly after the period
228 reported here). MSA shows very similar concentrations during spring and summer, and drops down to the limit
229 of detection level for autumn. Iodic acid acts very differently than the other compounds. We observe iodic acid
230 to have a similar level of concentration throughout the measurement period and the concentration almost seem
231 to “saturate” during daylight hours. This daytime maximum stays at the same level about 5 hours longer during
232 spring than in the autumn. The day length getting shorter towards the autumn explains this behavior. The
233 maximum hourly median concentrations for the measured compounds are $\sim 2 \cdot 10^6 \text{ cm}^{-3}$ for SA (spring), $\sim 5 \cdot$
234 10^5 cm^{-3} for MSA (summer), $\sim 3 \cdot 10^5 \text{ cm}^{-3}$ for iodic acid (all seasons) and $\sim 5 \cdot 10^7 \text{ cm}^{-3}$ for the sum of HOMs
235 (summer, mass range from 300 to 600 Th).

236 We can compare these numbers to SMEAR II long-term (5-year median concentration) observations, were the
237 median peak SA concentrations are $\sim 1.5 \cdot 10^6 \text{ cm}^{-3}$, $\sim 1 \cdot 10^6 \text{ cm}^{-3}$ and $\sim 3 \cdot 10^5 \text{ cm}^{-3}$ for spring, summer and
238 autumn, respectively (Sulo et al., 2021). These measured concentrations are very similar to SMEAR I
239 observations except a slightly higher summer and autumn SA concentration at SMEAR II. However, it should
240 be noted that the springtime measurements from SMEAR I do not include March data, which makes the
241 springtime comparison uncertain. There is also a difference in the timing of the peak SA concentration in the
242 summer. At SMEAR I the peak concentration is reached at noon and at SMEAR II it can be found some hours



243 earlier, already around eight o'clock in the morning (Sulo et al., 2021). In the case of HOMs, we cannot
244 compare the concentrations directly to Sulo et al. (2021) as they calculated the sum of HOMs differently, only
245 taking into account the most abundant signals and separating nitrate and non-nitrate HOMs. However, we take
246 the liberty to compare diurnal and seasonal variations. Both at SMEAR I and II, observations show the highest
247 HOM concentrations during summer, while the autumn concentrations are one order of magnitude lower. The
248 comparison between these sites reveals a different diurnal variation of HOMs. At SMEAR I, the HOMs have
249 a maximum around noon, spanning to the afternoon (Figure 3). At SMEAR II, HOMs have two maxima, one
250 at noon and another one in the early evening. From these, the latter is connected to non-nitrate monomer and
251 dimer HOMs and nitrate dimer HOMs. At SMEAR I the lack of an evening maximum could indicate that
252 HOM dimer formation is less dominant at SMEAR I compared to SMEAR II due to lower air temperatures,
253 or due to the different diurnal cycle of oxidants due to longer hours of solar radiation North of the Arctic Circle.

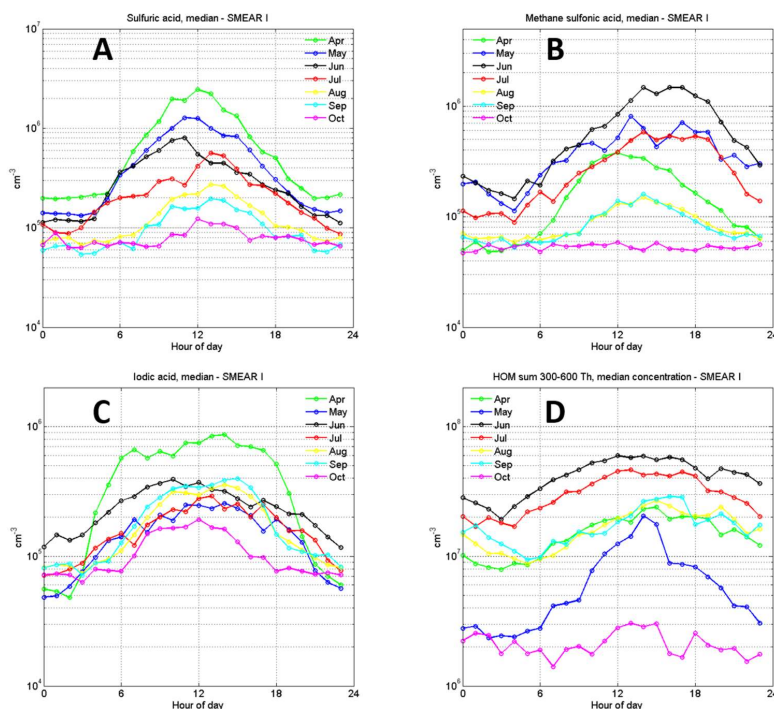
254



255

256 **Figure 3.** Diurnal variation of aerosol precursor gas median concentrations in different seasons: A) sulfuric
257 acid, B) methane sulfonic acid, C) iodic acid and d) the sum of HOMs in the 300 to 600 Th mass range.

258 When analyzing the monthly aerosol precursor profiles in Figure 4, we observe that the springtime atmosphere
259 is abundant in SA and iodic acid that have the highest median concentrations in April. MSA and HOMs
260 concentrations peak in June. The MSA behavior is likely connected to the algae blooms in the Arctic Ocean
261 that peak around midsummer. The marine emissions of DMS oxidize in the atmosphere to sulfur dioxide,
262 sulfuric acid and to MSA (e.g. Park et al., 2018). However, sulfuric acid has more sources, since SO₂, has also
263 anthropogenic sources. At SMEAR I we cannot distinguish these sources precisely (more discussion about this
264 in section 3.3.). It is notable that the peak concentration of MSA is earlier in the day in April, around 12 o'clock
265 noon, than it is later in the year when the peak concentration is reached in the late afternoon (from 13:00 to
266 18:00 o'clock). There are no previous MSA concentration reports from the SMEAR stations but some gas
267 phase MSA results from Antarctica show maximum of $1 \cdot 10^5 \text{ cm}^{-3}$ to $1 \cdot 10^7 \text{ cm}^{-3}$ concentrations (Mauldin et
268 al., 2004, Mauldin et al., 2010, Jokinen et al., 2018). In the Arctic, around half a year measurement series from
269 Villum in Greenland show MSA concentrations $< 10^6 \text{ cm}^{-3}$ (Mar – Sep) and from 10^5 cm^{-3} to 10^7 cm^{-3} with the
270 highest concentrations in June in Ny-Ålesund (Beck et al., 2021). Our measurements from the SMEAR I fall
271 in between these extremes.



272

273 **Figure 4.** Monthly median concentrations of A) sulfuric acid, B) methane sulfonic acid, C) iodic acid and d)
274 the sum of HOMs in the 300 to 600 Th mass range.

275 These are also the first reported results of iodic acid measurements from SMEAR I and they represent a
276 continental location, the White Sea coast being ~130 km South East and the Barents sea ~230 km to the North
277 East. Iodic acid, iodine and iodic oxoacid emissions are commonly connected to coastal or marine
278 environments (Baccarini et al., 2020; McFiggans et al., 2010; O’ Dowd et al., 2002; Sipilä et al., 2016; Yu et
279 al., 2019) due to the fact that the ocean surface is a major source of iodine (Carpenter et al., 2013). While it is
280 not precisely known how iodic acid forms in the gas phase, its formation requires oxidation of the initial
281 precursors (IO_x species) by ozone and the last steps of its formation is potentially driven by reaction with OH
282 (Chameides and Davis, 1980).

283 Compared to the other precursor compounds, iodic acid has the most stable concentration between seasons,
284 with a long increasing period in April during the snow-melting season. This is likely due to the simultaneously
285 increasing ozone concentrations (Fig 2B) and solar radiation. In contrast to measurements from the Arctic
286 Ocean (Baccarini et al., 2020), we did not observe a clear increase in iodic acid concentration in the autumn
287 due to freezing. We find that September had only marginally higher concentrations compared to August or
288 July (Fig 4). Winter measurements would be necessary to estimate the effect of freezing in the concentration
289 of IA.

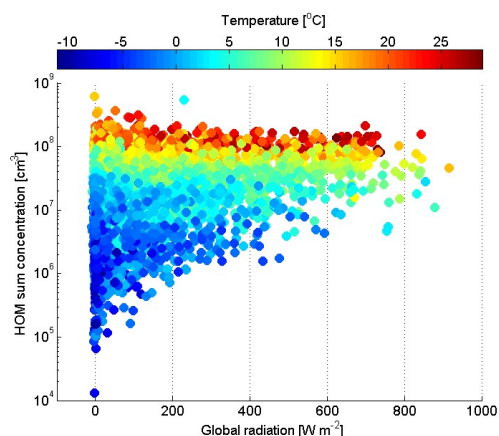
290 The source of iodic acid on a continental site like the SMEAR I is an interesting subject to speculate. The
291 observed HIO_3 peak in April could indicate that there could be an influence from air masses exposed to Arctic
292 marine environment, due to ocean surface acting as a major source of atmospheric iodine (Carpenter et al.,
293 2013). The increasing temperature in the spring induce a higher activity of phytoplankton in the nearby Barents
294 Sea and Norwegian Sea that remains ice free, even during the winter, and could result in the higher emission
295 of precursors for iodic acid (Lai et al., 2011). Higher temperature would also result in more efficient advection,
296 which would transport species faster from emission points to SMEAR I. The calculated back trajectories



297 support the idea that iodine-rich air masses arrive from the West or northwest to SMEAR I (discussed in details
298 in section 3.3. New Particle Formation evens and Figure 10). This would be the hypothesis of the long-range
299 transport for source of iodic acid in SMEAR I. On the contrary, the strong diurnal variation on iodic acid
300 concentration seen as one order of magnitude difference between noon and midnight, suggests fast on site
301 chemistry, which is not consistent with long-range transport. Also iodic acid life time against condensational
302 loss is expected to be short, in the range of an ~hour, this suggests that the source of HIO_3 is close to or at the
303 site of measurements. Land vegetation is a source of methyl iodide (CH_3I) that could be the source of iodic
304 acid at SMEAR I, at least during summer (Sive et al., 2007).

305 Most interestingly, we seem to have an emission source of iodine during all seasons. There are no reports on
306 iodine emissions from continental snow, but we hypothesize that one possible source of iodine in SMEAR I
307 during spring is the melting snowpack. This is possible due to the deposition of sea salts on snow particularly
308 during dark periods that activate during the spring and are re-emitted to the atmosphere through heterogeneous
309 photochemistry of iodide, and iodate ions (Raso et al., 2017; Spolaor et al., 2019). There are also possible
310 forest emissions of iodinated organics, similar to New England growing season (Raso et al., 2017), that might
311 be enhanced by higher temperature or high ozone concentrations. This type of emissions of iodinated gases,
312 or their implications, have not been studied before but these observations might direct research into emission
313 studies at SMEAR I, since our findings indicate that vegetation could be an emission source of iodine.

314 The sum of HOMs in SMEAR I reaches up to a median $\sim 5 \cdot 10^7 \text{ cm}^{-3}$ concentration in the summer. This is
315 about one order of magnitude lower than the concentrations reported from the SMEAR II station in Hyytiälä
316 (Yan et al., 2016), about 700 km south, where HOMs are at a maximum of $\sim 6 \cdot 10^8 \text{ cm}^{-3}$ during spring daytime.
317 It is striking how well the concentration of HOMs follow the air temperature (Figure 5). From the temperature
318 dependency, we can speculate that most VOCs emitted by vegetation close to Värriö could be monoterpenes
319 due to their strong temperature dependency. This is supported by emission rate measurements of VOCs
320 showing that in northern Finland 60 to 85 % are accounted by α - and β -pinene emissions (Tarvainen et al.,
321 2004). However, sesquiterpene emissions from nearby wetlands could contribute to HOMs since their
322 emissions are also temperature dependent and they are emitted by the boreal wetlands (Hellén et al., 2020;
323 Seco et al., 2020). As HOMs are oxidation products of VOCs, it is evident that the HOM concentration will
324 increase in SMEAR I in the future with the increasing VOC emissions, including isoprene, monoterpenes and
325 sesquiterpenes, due to temperature rise (Ghirardo et al., 2020; Tiiva et al., 2008; Valolahti et al., 2015).



326

327 **Figure 5.** HOM concentration (cm^{-3}) measured at SMEAR I (sum of mass range from 300 to 600 Th) as a
328 function of global radiation (W m^{-2}). The color in the plot represents air temperature in $^{\circ}\text{C}$. The plot includes
329 all data measured from April to October 2019.

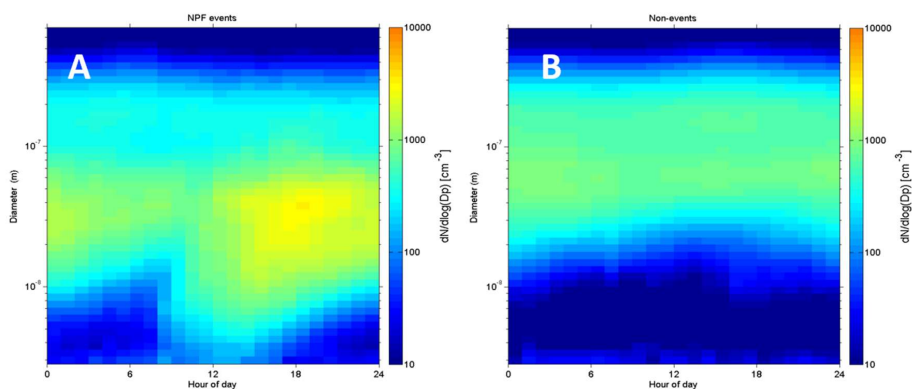
330



331 **New particle formation events;**

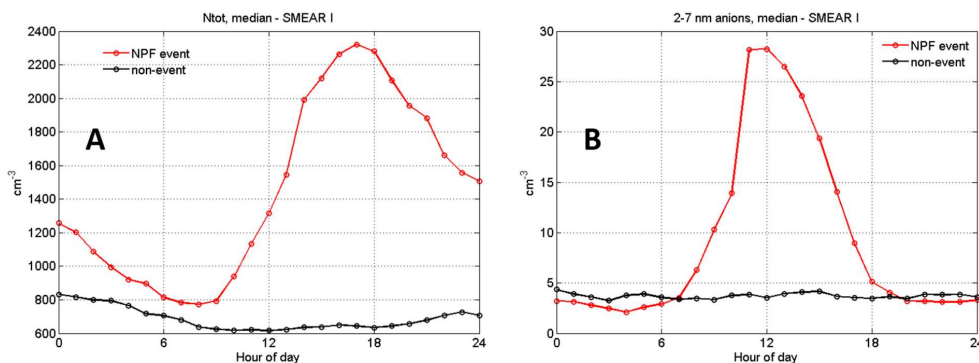
332 During the measurement period from 4 April 2019 to 27 October 2019, we observed 36 regional NPF events
333 in total and our CI-API-TOF data covers 33 of these NPF days. During the same period, we observed 75 non-
334 event days without clear signs of particle formation (Dal Maso et al., 2005). Rest of the days during our
335 measurement period were defined as undefined, bad data or partly bad data days and these were excluded from
336 our analysis. In this chapter, we focus on trace gases, meteorological parameters and aerosol precursor detected
337 gases during NPF days and compare them to non-event days.

338 We plot NPF and non-event days median average number size distribution of aerosol particles (from 3 to 800
339 nm) in Figure 6, and the total number concentration and the 2-7 nm air ion concentrations in Figure 7. In figure
340 6, in the case of NPF event days we see a distinct “banana” plot, where small < 10 nm, particles are forming
341 and growing with time. The DMPS data is plotted from 2.82 nm to 708 nm but note that the channels below
342 ~5 nm have much larger uncertainties than those above. The median event start time is located around noon
343 and the growth of particles continues steadily until midnight. However, when looking at individual days, there
344 is a large variation in the start-times of the particle formation, some events start early in the morning or even
345 in the night, while some start in late afternoon. Non-event days show very few particles in the < 10 nm size
346 bins.



347

348 **Figure 6.** This figure depicts the median number size distribution during all observed during NPF events ($n =$
349 33) and non-events ($n = 75$) during our measurement period. The data is collected with a DMPS and size bins
350 from 2.82 to 708 nm are plotted.



351

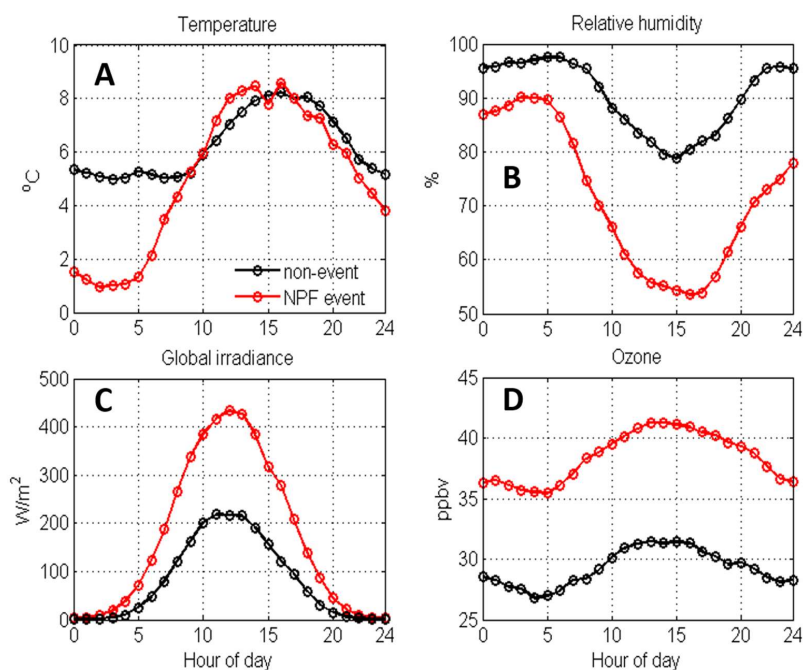
352



353 **Figure 7.** Median total particle concentration (N_{tot}) in A) and 2-7 nm negative ion concentrations in B) at
354 SMEAR I during NPF event (red, n = 33) and non-event days (black, n = 75). The total particle number
355 concentration is recorded with a CPC and air ion concentrations with a NAIS.

356 The total number of particles measured at the site during NPF events rises up to ~2400 cm⁻³ reaching the
357 maximum concentration at ~17 o'clock in the evening. This shows that NPF is an important source of aerosol
358 particles in Värriö as previously reported (Vehkamäki et al., 2004). Non-event days have clearly lower particle
359 concentrations throughout the day, staying lower than 1000 cm⁻³ on average. The measured 2-7 nm anion
360 concentrations stay very low during non-event days. As intermediate ions form mainly during NPF, their
361 concentrations are used as indicator of NPF events in boreal environments (Leino et al., 2016). On NPF days,
362 we see a peak in the anion concentration at noon, the concentration being about six times higher than during
363 non-event days. This indicates that negative ions may play a role in SMEAR I particle formation events.

364 Figure 8 shows the differences in temperature, relative humidity, global radiation and ozone concentration
365 between NPF event days (in red) and non-event days (black). In Värriö, NPF events preferably happen in
366 relatively low temperatures with a fast temperature rise in the early morning hours, lower and decreasing RH
367 during the NPF days compared to non-event days. NPF days have clearly higher global irradiance values and
368 about 10 ppbv higher ozone concentrations than non-event days. The meteorological conditions favoring NPF
369 are thus similar than at the SMEAR II station in Hyytiälä, where sunny clear sky days with low RH and
370 condensation sink along with wind directions from the cleaner northerly sector are forecasting NPF events
371 (Nieminen et al., 2014).



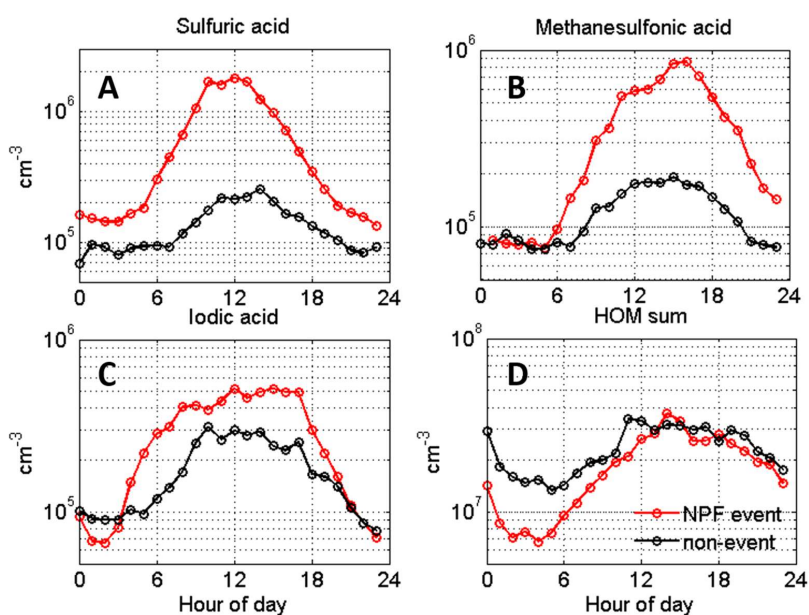
372

373 **Figure 8.** Average temperature (°C) in panel A), relative humidity (%) in B), global radiation (W m⁻²) in C)
374 and ozone concentration (ppbv) in D), all measured at SMEAR I during NPF event (red, n = 33) and non-event
375 days (black, n = 75).

376 Next, we show the concentrations of aerosol precursor compounds during NPF and non-event days in figure
377 9. (Kulmala et al., 2013)The sulfuric acid concentrations closely follow the solar irradiation profile (Figure 8).



378 Similarly to the results obtained from the high Arctic, Svalbard, also MSA is elevated during NPF events,
379 especially during summer, and could possibly contribute aerosol growth (Beck et al., 2021). We observe close
380 to an order of magnitude higher MSA concentration between the events and non-events days, highlighting the
381 dominant role of sulfur species to nucleation and growth in general at this site. In order to attribute the source
382 of sulfur species and IA during the event and non-event days we performed a cluster analysis using a
383 geographical information system (GIS) based software, Trajstat (Wang et al., 2009). The NCEP/NCAR
384 reanalysis data was used as meteorological input for the model (Kalnay et al., 1996). The simulations were
385 performed at an arrival height of 250 m. a.g.l. SMEAR I station is located approximately at similar height (390
386 m a.s.l), thus representing the air masses arriving at the station even during strong temperature inversions
387 (Sipilä et al., 2021).



388

389 **Figure 9.** Aerosol precursor gases in SMEAR I during NPF (red, $n = 33$) and non-event days (black, $n = 75$).
390 The data is hourly median average.

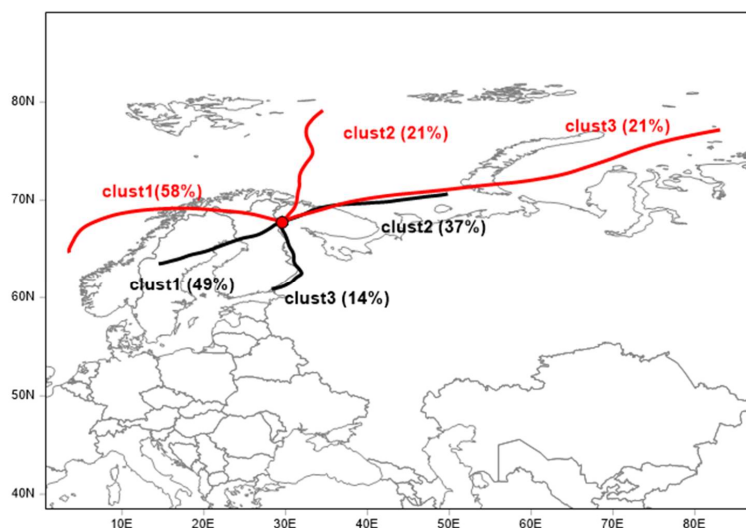
391 Higher concentrations of aerosol precursors SA, MSA and IA are connected to the air masses that arrive to
392 SMEAR I from the Arctic Ocean (Figure 10). Cluster analysis of air mass back trajectories arriving to Värriö
393 during NPF days clearly shows, that most NPF events occur when the air mass was exposed to marine
394 environments within the last 72 hours. In our case, mainly the Norwegian Sea in the West (58 %) or the Barents
395 (21 %) and Kara Seas (21 %) in the Arctic Ocean. This seems relevant to our results since the marine
396 environment in the North is emitting large amounts of dimethyl sulfide (DMS), a precursor for SA and MSA
397 (Levasseur, 2013) and iodine species that further oxidize to IA (Baccarini et al., 2020; Sherwen et al., 2016).
398 A fraction of air masses that are connected to both NPF (21 %) and non-event days (37 %) are coming to
399 SMEAR I from the Kola peninsula that is connected to high SO_2 emissions, higher particle number
400 concentrations and winter time NPF events (Sipilä et al., 2021). Most non-event air masses arrive to Värriö
401 from South-West (49 %) crossing northern Finland and Sweden.

402 In addition from Figure 9 we observe that we cannot rule out the contribution of iodic acid in NPF in SMEAR
403 I, but with the recorded concentration, it usually is not enough to initiate NPF (He et al., 2021). Although iodic
404 acid concentrations are slightly larger on NPF days than non-event days, the rise in concentration happens
405 already early in the morning, clearly before the average event start-time. The possible source of iodic acid was



406 discussed earlier in chapter 3.2 and we hypothesize that the source of iodine at SMEAR I could be both; i) the
407 long distance transport from the Arctic Ocean combined to ii) the local emissions from the snow pack and
408 vegetation. The hypothesis of vegetation emitted iodine species is supported by the minor difference between
409 NPF (mostly marine) and non-event day (mostly continental) concentrations. At SMEAR I, HOMs are the
410 only species that are at a (marginally) lower level during non-event than NPF days indicating that the total
411 HOM concentration does not determine when NPF events occur. However, this does not exclude the possible
412 participation of certain HOMs in NPF together with sulfur compounds (Lehtipalo et al., 2018) or at later stages
413 of the NPF process, especially during particle growth. However, pure biogenic nucleation involving ions and
414 HOMs (Kirkby et al., 2016) seems not to be a major NPF pathway in Värriö.

415 Our measurements do not unveil the detailed mechanism of nucleation or growth of particles. We lack
416 measurements of ambient bases that are needed to stabilize sulfuric acid clusters in ambient conditions (e.g.
417 Almeida et al., 2013; Jen et al., 2014; Kirkby et al., 2011; Kürten et al., 2014; Myllys et al., 2018). With the
418 given observations comparing NPF days with non-event days it is likely that most regional NPF events require
419 sulfuric acid, but the NPF process can involve other compounds as well, especially IA and MSA, which show
420 higher concentrations on NPF days, very similarly that the results reported from Ny-Ålesund (Beck et al.,
421 2021).



422

423 **Figure 10.** Trajectory cluster analysis of 72-hour back trajectories simulated at arrival height of 250 m a.g.l.
424 and the NCEP/NCAR reanalysis data used as meteorological input. Red = NPF event, black = non-NPF

425 **Conclusions:**

426 We report ~7 months of nitrate based CI-APi-TOF measurements of sulfuric acid, methane sulfonic acid, iodic
427 acid and highly oxygenated organic compounds from a remote sub-Arctic field station SMEAR I in Finland.
428 The measurements aim to increase our understanding of the Arctic aerosol forming precursors and atmospheric
429 chemistry in more detail. The reason for measuring these compounds ~150 km north of the Arctic Circle is
430 simple; the Arctic is warming twice the speed as the planet on average. Lapland is already facing environmental
431 changes when e.g. woody plants disperse further north and influence the tundra ecosystem (Aakala et al., 2014;
432 Kemppinen et al., 2021). These changes will in turn affect the emissions of aerosol precursor gases, which
433 may have feedback effects on to the climate (e.g. Kulmala et al., 2020; Paasonen et al., 2013).



434 The area surrounding SMEAR I station has snow cover for almost 8 months a year. Accumulating snow during
435 the autumn is a good reservoir to e.g. halogens, similarly than in the high Arctic (and Arctic Ocean)
436 environment. The snow pack also acts as a cover for biogenic emissions entering the atmosphere from the
437 ground. Any changes in the temperature and snow cover in the sub-Arctic regions will effect on atmospheric
438 chemistry and composition that are undeniably changing the way aerosol particles form and what their number
439 concentration is in the region.

440 In this study, we report seasonal and monthly variations of SA, MSA, IA and HOM concentrations and find
441 all these compounds abundant in springtime. SA has a peak concentration in the spring, decreasing for the rest
442 of the seasons. We detect high concentrations of MSA and IA that are usually connected to marine and coastal
443 environments, although Värriö is located ~130 km from the nearest coast of the White Sea. While MSA is
444 abundant in the spring, summer and decreases to limit of detection levels for autumn, IA continues at the same
445 concentration throughout the seasons. It seems likely that these two compounds are connected to emissions
446 from phytoplankton or the Arctic ice pack and arrive to SMEAR I by long transport routes. In the case of iodic
447 acid, we suggest that the source of iodine emissions is a combination of transport and local emission from the
448 continental snow pack and vegetation at the site. Further work is needed to confirm this hypothesis.

449 The most striking correlation we found in HOM concentrations and ambient air temperature. The vegetation
450 at SMEAR I is the source of VOCs even in the snow covered spring season and these volatile gases are oxidized
451 into HOMs with different reaction rates depending on the oxidant. In the case of such strong temperature
452 controlled HOM concentrations, we conclude that HOMs in the mass range of 300 – 600 Th are most likely
453 products of monoterpene oxidation.

454 We also studied the abundance of these aerosol precursors separately during NPF and non-event days. We
455 observed that new particles at SMEAR I preferably form in relatively low temperatures (< 10°C), low relative
456 humidity that decreases with rising temperature during the day, ~10 ppbv higher ozone concentration than
457 during non-event days, high SA concentration in the morning and high MSA concentrations in the afternoon.
458 Cluster analysis of air masses show that NPF usually happens in marine air masses travelling to the site from
459 North west - West. All together, these are the first long term measurements of aerosol forming precursor from
460 the sub-arctic region helping us to understand atmospheric chemical processes and aerosol formation in the
461 rapidly changing Arctic.

462 **Data availability:**

463 All meteorological parameters, trace gas concentrations and aerosol data we downloaded directly from
464 smartSMEAR open access database (<https://smear.avaa.csc.fi/>). All mass spectrometric data are available on
465 request from the corresponding author.

466 **Author contribution:**

467 TJ, MS, TP and MK designed the experiments at SMEAR III and MS, NS, KN and TL carried them out. IY
468 made the NPF event analysis and RT calculated the back trajectories. TJ and KL wrote the manuscript with
469 contributions from all co-authors.

470 **Competing interests:**

471 Markku Kulmala is editor of ACP. Tuukka Petäjä is editor of ACP.

472 **Acknowledgements:**

473 We would like to thank the technical staff in Kumpula and Värriö, who keep the long-term measurements
474 going and helped with data collection, instrument calibrations, logistics and in data quality control and
475 assurance during the year. We acknowledge the important role our collaborators have in scientific discussion
476 and a special thanks goes to Alfonso Saiz-Lopez for iodic acid related discussion that helped to draft this



477 article. We thank the ACTRIS CiGas-UHEL unit for mass spectrometer calibration support and the tofTools
478 team for data analysis software.

479 **Financial support:**

480 The Academy of Finland via Center of Excellence in Atmospheric Sciences (project no. 272041) and European
481 Research Council via ATM-GTP 266 (742206), GASPARCON (714621) and Flagship funding (grant no. 1235656,
482 337549) funded this work. We also received funding from the Academy of Finland (project no. 1235656,
483 296628, 316114, 315203, 307537, 325647, 33397, 334792 and 334514) “Quantifying carbon sink,
484 CarbonSink+ and their interaction with air quality” and Academy professorship (grant no. 302958). This work
485 was further supported by the European Commission via via project iCUPE (Integrative and Comprehensive
486 Understanding on Polar Environments, No 689443), the EMME-CARE project which received funding from
487 the European Union's Horizon 2020 Research and Innovation Programme, under grant agreement no. 856612,
488 Regional Council of Lapland (Väriön tutkimuskeskustuksen huippuututkimus hyödyntämään Itä-Lapin
489 elinkeinoelämää, VÄRI, A74190) and Aatos Erkkö Foundation.

490 **References:**

- 491 Aakala, T., Hari, P., Dengel, S., Newberry, S. L., Mizunuma, T. and Grace, J.: A prominent stepwise
492 advance of the tree line in north-east Finland, *J. Ecol.*, 102(6), 1582–1591, doi:10.1111/1365-2745.12308,
493 2014.
- 494 Ahonen, T., Aalto, P., Rannik, Ü., Kulmala, M., Nilsson, E. D., Palmroth, S., Ylitalo, H. and Hari, P.:
495 Variations and vertical profiles of trace gas and aerosol concentrations and CO₂ exchange in eastern
496 Lapland, *Atmos. Environ.*, 31(20), 3351–3362, doi:10.1016/S1352-2310(97)00151-9, 1997.
- 497 Almeida, J., Schobesberger, S., Kürten, A., Ortega, I. K., Kupiainen-Määttä, O., Praplan, A. P., Adamov, A.,
498 Amorim, A., Bianchi, F., Breitenlechner, M., David, A., Dommen, J., Donahue, N. M., Downard, A., Dunne,
499 E., Duplissy, J., Ehrhart, S., Flagan, R. C., Franchin, A., Guida, R., Hakala, J., Hansel, A., Heinritzi, M.,
500 Henschel, H., Jokinen, T., Junninen, H., Kajos, M., Kangasluoma, J., Keskinen, H., Kupc, A., Kurtén, T.,
501 Kvashin, A. N., Laaksonen, A., Lehtipalo, K., Leiminger, M., Leppä, J., Loukonen, V., Makhmutov, V.,
502 Mathot, S., McGrath, M. J., Nieminen, T., Olenius, T., Onnela, A., Petäjä, T., Riccobono, F., Riipinen, I.,
503 Rissanen, M., Rondo, L., Ruuskanen, T., Santos, F. D., Sarnela, N., Schallhart, S., Schnitzhofer, R., Seinfeld,
504 J. H., Simon, M., Sipilä, M., Stozhkov, Y., Stratmann, F., Tomé, A., Tröstl, J., Tsagkogeorgas, G.,
505 Vaattovaara, P., Viisanen, Y., Virtanen, A., Vrtala, A., Wagner, P. E., Weingartner, E., Wex, H.,
506 Williamson, C., Wimmer, D., Ye, P., Yli-Juuti, T., Carslaw, K. S., Kulmala, M., Curtius, J., Baltensperger,
507 U., Worsnop, D. R., Vehkamäki, H. and Kirkby, J.: Molecular understanding of sulphuric acid-amine
508 particle nucleation in the atmosphere, *Nature*, 502(7471), 359–363, doi:10.1038/nature12663, 2013.
- 509 Baccarini, A., Karlsson, L., Dommen, J., Duplessis, P., Vüllers, J., Brooks, I. M., Saiz-Lopez, A., Salter, M.,
510 Tjernström, M., Baltensperger, U., Zieger, P. and Schmale, J.: Frequent new particle formation over the high
511 Arctic pack ice by enhanced iodine emissions, *Nat. Commun.*, 11(1), doi:10.1038/s41467-020-18551-0,
512 2020.
- 513 Beck, L. J., Sarnela, N., Junninen, H., Hoppe, C. J. M., Garmash, O., Bianchi, F., Riva, M., Rose, C.,
514 Peräkylä, O., Wimmer, D., Kausiala, O., Jokinen, T., Ahonen, L., Mikkilä, J., Hakala, J., He, X. C.,
515 Kontkanen, J., Wolf, K. K. E., Cappelletti, D., Mazzola, M., Traversi, R., Petroselli, C., Viola, A. P., Vitale,
516 V., Lange, R., Massling, A., Nøjgaard, J. K., Krejci, R., Karlsson, L., Zieger, P., Jang, S., Lee, K., Vakkari,
517 V., Lampilahti, J., Thakur, R. C., Leino, K., Kangasluoma, J., Duplissy, E. M., Siivola, E., Marbouti, M.,
518 Tham, Y. J., Saiz-Lopez, A., Petäjä, T., Ehn, M., Worsnop, D. R., Skov, H., Kulmala, M., Kerminen, V. M.
519 and Sipilä, M.: Differing Mechanisms of New Particle Formation at Two Arctic Sites, *Geophys. Res. Lett.*,
520 48(4), doi:10.1029/2020GL091334, 2021.
- 521 Berndt, T., Richters, S., Jokinen, T., Hyttinen, N., Kurtén, T., Otkjær, R. V., Kjaergaard, H. G., Stratmann,
522 F., Herrmann, H., Sipilä, M., Kulmala, M. and Ehn, M.: Hydroxyl radical-induced formation of highly
523 oxidized organic compounds, *Nat. Commun.*, 7, 13677, doi:10.1038/ncomms13677, 2016.



- 524 Bianchi, F., Garmash, O., He, X., Yan, C., Iyer, S., Rosendahl, I., Xu, Z., Rissanen, M. P., Riva, M., Taipale,
525 R., Sarnela, N., Petäjä, T., Worsnop, D. R., Kulmala, M., Ehn, M. and Junninen, H.: The role of highly
526 oxygenated molecules (HOMs) in determining the composition of ambient ions in the boreal forest, *Atmos.*
527 *Chem. Phys.*, 17(22), 13819–13831, doi:10.5194/acp-17-13819-2017, 2017.
- 528 Bradshaw, C. J. A. and Warkentin, I. G.: Global estimates of boreal forest carbon stocks and flux, *Glob.*
529 *Planet. Change*, 128, 24–30, doi:10.1016/j.gloplacha.2015.02.004, 2015.
- 530 Brandt, J. P., Flannigan, M. D., Maynard, D. G., Thompson, I. D. and Volney, W. J. A.: An introduction to
531 Canada's boreal zone: Ecosystem processes, health, sustainability, and environmental issues I, *Environ. Rev.*,
532 21(4), 207–226, doi:10.1139/er-2013-0040, 2013.
- 533 Carpenter, L. J., MacDonald, S. M., Shaw, M. D., Kumar, R., Saunders, R. W., Parthipan, R., Wilson, J. and
534 Plane, J. M. C.: Atmospheric iodine levels influenced by sea surface emissions of inorganic iodine, *Nat.*
535 *Geosci.*, 6(2), 108–111, doi:10.1038/ngeo1687, 2013.
- 536 Chameides, W. L. and Davis, D. D.: Iodine: Its possible role in tropospheric photochemistry, *J. Geophys.*
537 *Res. Ocean.*, 85(C12), 7383–7398, doi:10.1029/JC085IC12P07383, 1980.
- 538 Charlson, R. J., Lovelock, J. E., Andreae, M. O. and Warren, S. G.: Oceanic phytoplankton, atmospheric
539 sulphur, cloud albedo and climate, *Nature*, 326(6114), 655–661, doi:10.1038/326655a0, 1987.
- 540 Dal Maso, M., Kulmala, M., Riipinen, I., Wagner, R., Hussein, T., Aalto, P. P. and Lehtinen, K. E. J.:
541 Formation and growth of fresh atmospheric aerosols: Eight years of aerosol size distribution data from
542 SMEAR II, Hyytiälä, Finland, *Boreal Environ. Res.*, 10(5), 323–336, 2005.
- 543 Dal Maso, M., Sogacheva, L., Aalto, P. P., Riipinen, I., Komppula, M., Tunved, P., Korhonen, L., Suur-Uski,
544 V., Hirsikko, A., Kurtén, T., Kerminen, V.-M., Lihavainen, H., Viisanen, Y., Hansson, H.-C., Kulmala, M.,
545 Aerosol size distribution measurements at four Nordic field stations: identification, analysis and trajectory
546 analysis of new particle formation bursts, *Tellus B: Chemical and Physical meteorology*, 59(3), 350–361,
547 doi:10.1111/j.1600-0889.2007.00267.x, 2007.
- 548 Dall'Osto, M., Geels, C., Beddows, D. C. S., Boertmann, D., Lange, R., Nøjgaard, J. K., Harrison, R. M.,
549 Simo, R., Skov, H. and Massling, A.: Regions of open water and melting sea ice drive new particle formation
550 in North East Greenland., *Sci. Rep.*, 8(1), 6109, doi:10.1038/s41598-018-24426-8, 2018.
- 551 Ehn, M., Thornton, J. A., Kleist, E., Sipilä, M., Junninen, H., Pullinen, I., Springer, M., Rubach, F.,
552 Tillmann, R., Lee, B., Lopez-Hilfiker, F., Andres, S., Acir, I.-H. H., Rissanen, M., Jokinen, T.,
553 Schobesberger, S., Kangasluoma, J., Kontkanen, J., Nieminen, T., Kurtén, T., Nielsen, L. B., Jørgensen, S.,
554 Kjaergaard, H. G., Canagaratna, M., Maso, M. D., Berndt, T., Petäjä, T., Wahner, A., Kerminen, V.-M. M.,
555 Kulmala, M., Worsnop, D. R., Wildt, J. and Mentel, T. F.: A large source of low-volatility secondary organic
556 aerosol, *Nature*, 506(7489), 476–479, doi:10.1038/nature13032, 2014.
- 557 Ghirardo, A., Lindstein, F., Koch, K., Buegger, F., Schloter, M., Albert, A., Michelsen, A., Winkler, J. B.,
558 Schnitzler, J.-P. and Rinnan, R.: Origin of volatile organic compound emissions from subarctic tundra under
559 global warming, *Glob. Chang. Biol.*, 26(3), 1908–1925, doi:10.1111/GCB.14935, 2020.
- 560 Hari, P., Aalto, P., Hämeri, K., Kulmala, M., Lahti, T., Luoma, S., Palva, L., Pohja, T., Pulliainen, E.,
561 Siivola, E. and Vesala, T.: Air pollution in eastern Lapland: challenge for an environmental measurement
562 station, *Silva Fenn.*, 28(1), 29–39, doi:10.14214/SF.A9160, 1994.
- 563 He, X.-C., Tham, Y. J., Dada, L., Wang, M., Finkenzeller, H., Stolzenburg, D., Iyer, S., Simon, M., Kürten,
564 A., Shen, J., Rörup, B., Rissanen, M., Schobesberger, S., Baalbaki, R., Wang, D. S., Koenig, T. K., Jokinen,
565 T., Sarnela, N., Beck, L. J., Almeida, J., Amanatidis, S., Amorim, A., Ataei, F., Baccarini, A., Bertozzi, B.,
566 Bianchi, F., Brilke, S., Caudillo, L., Chen, D., Chiu, R., Chu, B., Dias, A., Ding, A., Dommen, J., Duplissy,
567 J., Haddad, I. El, Carracedo, L. G., Granzin, M., Hansel, A., Heinritzi, M., Hofbauer, V., Junninen, H.,
568 Kangasluoma, J., Kemppainen, D., Kim, C., Kong, W., Krechmer, J. E., Kvashin, A., Laitinen, T.,
569 Lamkaddam, H., Lee, C. P., Lehtipalo, K., Leiminger, M., Li, Z., Makhmutov, V., Manninen, H. E., Marie,
570 G., Marten, R., Mathot, S., Mauldin, R. L., Mentler, B., Möhler, O., Müller, T., Nie, W., Onnela, A., Petäjä,



- 571 T., Pfeifer, J., Philippov, M., Ranjithkumar, A., Saiz-Lopez, A., Salma, I., Scholz, W., Schuchmann, S.,
572 Schulze, B., Steiner, G., Stozhkov, Y., Tauber, C., Tomé, A., Thakur, R. C., Väisänen, O., Vazquez-Pufleau,
573 M., Wagner, A. C., Wang, Y., Weber, S. K., Winkler, P. M., Wu, Y., Xiao, M., Yan, C., Ye, Q., Ylisirniö,
574 A., Zauner-Wieczorek, M., Zha, Q., Zhou, P., Flagan, R. C., Curtius, J., Baltensperger, U., Kulmala, M.,
575 Kerminen, V.-M., Kurtén, T., et al.: Role of iodine oxoacids in atmospheric aerosol nucleation, *Science*,
576 371(6529), 589–595, doi:10.1126/SCIENCE.ABE0298, 2021.
- 577 Hellén, H., Schallhart, S., Praplan, A. P., Tykkä, T., Aurela, M., Lohila, A., and Hakola, H.: Sesquiterpenes
578 dominate monoterpenes in northern wetland emissions, *Atmos. Chem. Phys.*, 20, 7021–7034,
579 <https://doi.org/10.5194/acp-20-7021-2020>, 2020.
- 580 Hyttinen, N., Kupiainen-Määttä, O., Rissanen, M. P., Muuronen, M., Ehn, M. and Kurtén, T.: Modeling the
581 Charging of Highly Oxidized Cyclohexene Ozonolysis Products Using Nitrate-Based Chemical Ionization, *J.*
582 *Phys. Chem. A*, 119(24), 6339–6345, doi:10.1021/acs.jpca.5b01818, 2015.
- 583 IPCC, F. assessment report: Fifth Assessment Report - Climate Change 2013, IPCC, Fifth Assess. Rep. -
584 Clim. Chang. [online] Available from: <http://www.ipcc.ch/report/ar5/wg1/> (Accessed 3 February 2016),
585 2013.
- 586 Jen, C. N., McMurry, P. H. and Hanson, D. R.: Stabilization of sulfuric acid dimers by ammonia,
587 methylamine, dimethylamine, and trimethylamine, *J. Geophys. Res. Atmos.*, 119(12), 7502–7514,
588 doi:10.1002/2014JD021592, 2014.
- 589 Jokinen, T., Sipilä, M., Junninen, H., Ehn, M., Lönn, G., Hakala, J., Petäjä, T., Mauldin, R. L., Kulmala, M.
590 and Worsnop, D. R.: Atmospheric sulphuric acid and neutral cluster measurements using CI-API-TOF,
591 *Atmos. Chem. Phys.*, 12(9), 4117–4125, doi:10.5194/acp-12-4117-2012, 2012.
- 592 Jokinen, T., Sipilä, M., Richters, S., Kerminen, V.-M. M., Paasonen, P., Stratmann, F., Worsnop, D.,
593 Kulmala, M., Ehn, M., Herrmann, H. and Berndt, T.: Rapid Autoxidation Forms Highly Oxidized RO 2
594 Radicals in the Atmosphere, *Angew. Chemie Int. Ed.*, 53(52), 14596–14600, doi:10.1002/anie.201408566,
595 2014.
- 596 Jokinen, T., Kontkanen, J., Lehtipalo, K., Manninen, H. E., Aalto, J., Porcar-Castell, A., Garmash, O.,
597 Nieminen, T., Ehn, M., Kangasluoma, J., Junninen, H., Levula, J., Duplissy, J., Ahonen, L. R., Rantala, P.,
598 Heikkinen, L., Yan, C., Sipilä, M., Worsnop, D. R., Bäck, J., Petäjä, T., Kerminen, V.-M. and Kulmala, M.:
599 Solar eclipse demonstrating the importance of photochemistry in new particle formation., *Sci. Rep.*, 7,
600 45707, doi:10.1038/srep45707, 2017.
- 601 Junninen, H., Ehn, M., Petäjä, T., Luosujärvi, L., Kotiaho, T., Kostianen, R., Rohner, U., Gonin, M., Fuhrer,
602 K., Kulmala, M. and Worsnop, D. R.: A high-resolution mass spectrometer to measure atmospheric ion
603 composition, *Atmos. Meas. Tech.*, 3(4), 1039–1053, doi:10.5194/amt-3-1039-2010, 2010.
- 604 Kalnay, E., Kanamitsu, M., Kistler, R., Collins, W., Deaven, D., Gandin, L. and E. Kalnay M. Kanamitsu R.
605 Kistler W. Collins D. Deaven L. Gandin M. Iredell S. Saha G. White J. Woollen Y. Zhu M. Chelliah W.
606 Ebisuzaki W. HE. Kalnay M. Kanamitsu R. Kistler W. Collins D. Deaven L. Gandin M. Iredell S. Saha G.
607 White, and D. J.: The NCEP/NCAR 40-Year Reanalysis Project, *Bull. Am. Meteorol. Soc.*, 437–472,
608 doi:[https://doi.org/10.1175/1520-0477\(1996\)077<0437:TNYRP>2.0.CO;2](https://doi.org/10.1175/1520-0477(1996)077<0437:TNYRP>2.0.CO;2), 1996.
- 609 Kempainen, J., Niittynen, P., Virkkala, A.-M., Happonen, K., Riihimäki, H., Aalto, J. and Luoto, M.: Dwarf
610 Shrubs Impact Tundra Soils: Drier, Colder, and Less Organic Carbon, *Ecosyst.* 2021, 1–15,
611 doi:10.1007/S10021-020-00589-2, 2021.
- 612 Kerminen, V.-M., Paramonov, M., Anttila, T., Riipinen, I., Fountoukis, C., Korhonen, H., Asmi, E., Laakso,
613 L., Lihavainen, H., Swietlicki, E., Svenningsson, B., Asmi, A., Pandis, S. N., Kulmala, M. and Petäjä, T.:
614 Cloud condensation nuclei production associated with atmospheric nucleation: a synthesis based on existing
615 literature and new results, *Atmos. Chem. Phys.*, 12(24), 12037–12059, doi:10.5194/acp-12-12037-2012,
616 2012.
- 617 Kerminen, V., Aurela, M., Hillamo, R. E. and Virkkula, A.: Formation of particulate MSA: deductions from



- 618 size distribution measurements in the Finnish Arctic, *Tellus B*, 49(2), 159–171, doi:10.1034/j.1600-
619 0889.49.issue2.4.x, 1997.
- 620 Kirkby, J., Curtius, J., Almeida, J., Dunne, E., Duplissy, J., Ehrhart, S., Franchin, A., Gagné, S., Ickes, L.,
621 Kürten, A., Kupc, A., Metzger, A., Riccobono, F., Rondo, L., Schobesberger, S., Tsagkogeorgas, G.,
622 Wimmer, D., Amorim, A., Bianchi, F., Breitenlechner, M., David, A., Dommen, J., Downard, A., Ehn, M.,
623 Flagan, R. C., Haider, S., Hansel, A., Hauser, D., Jud, W., Junninen, H., Kreissl, F., Kvashin, A., Laaksonen,
624 A., Lehtipalo, K., Lima, J., Lovejoy, E. R., Makhmutov, V., Mathot, S., Mikkilä, J., Minginette, P., Mogo,
625 S., Nieminen, T., Onnela, A., Pereira, P., Petäjä, T., Schnitzhofer, R., Seinfeld, J. H., Sipilä, M., Stozhkov,
626 Y., Stratmann, F., Tomé, A., Vanhanen, J., Viisanen, Y., Virtala, A., Wagner, P. E., Walther, H.,
627 Weingartner, E., Wex, H., Winkler, P. M., Carslaw, K. S., Worsnop, D. R., Baltensperger, U. and Kulmala,
628 M.: Role of sulphuric acid, ammonia and galactic cosmic rays in atmospheric aerosol nucleation., *Nature*,
629 476(7361), 429–433, doi:10.1038/nature10343, 2011.
- 630 Kirkby, J., Duplissy, J., Sengupta, K., Frege, C., Gordon, H., Williamson, C., Heinritzi, M., Simon, M., Yan,
631 C., Almeida, J. J., Trostl, J., Nieminen, T., Ortega, I. K., Wagner, R., Adamov, A., Amorim, A.,
632 Bernhammer, A.-K. K., Bianchi, F., Breitenlechner, M., Brilke, S., Chen, X., Craven, J., Dias, A., Ehrhart,
633 S., Flagan, R. C., Franchin, A., Fuchs, C., Guida, R., Hakala, J., Hoyle, C. R., Jokinen, T., Junninen, H.,
634 Kangasluoma, J., Kim, J., Krapf, M., Kurten, A., Laaksonen, A., Lehtipalo, K., Makhmutov, V., Mathot, S.,
635 Molteni, U., Onnela, A., Perakyla, O., Piel, F., Petaja, T., Praplan, A. P., Pringle, K., Rap, A., Richards, N.
636 A. D. D., Riipinen, I., Rissanen, M. P., Rondo, L., Sarnela, N., Schobesberger, S., Scott, C. E., Seinfeld, J.
637 H., Sipilä, M., Steiner, G., Stozhkov, Y., Stratmann, F., Tomé, A., Virtanen, A., Vogel, A. L., Wagner, A. C.,
638 Wagner, P. E., Weingartner, E., Wimmer, D., Winkler, P. M., Ye, P., Zhang, X., Hansel, A., Dommen, J.,
639 Donahue, N. M., Worsnop, D. R., Baltensperger, U., Kulmala, M., Carslaw, K. S., Curtius, J., Tröstl, J.,
640 Nieminen, T., Ortega, I. K., Wagner, R., Adamov, A., Amorim, A., Bernhammer, A.-K. K., Bianchi, F.,
641 Breitenlechner, M., Brilke, S., Chen, X., Craven, J., Dias, A., Ehrhart, S., Flagan, R. C., Franchin, A., Fuchs,
642 C., Guida, R., Hakala, J., Hoyle, C. R., Jokinen, T., et al.: Ion-induced nucleation of pure biogenic particles,
643 *Nature*, 533(7604), 521–526, doi:10.1038/nature17953, 2016.
- 644 Kulmala, M., Toivonen, A., Mäkelä, J. M. and Laaksonen, A.: Analysis of the growth of nucleation mode
645 particles observed in Boreal forest, *Tellus B*, 50(5), 449–462, doi:10.1034/j.1600-0889.1998.t01-4-00004.x,
646 1998.
- 647 Kulmala, M., Riipinen, I., Sipilä, M., Manninen, H. E., Petäjä, T., Junninen, H., Dal Maso, M., Mordas, G.,
648 Mirme, A., Vana, M., Hirsikko, A., Laakso, L., Harrison, R. M., Hanson, I., Leung, C., Lehtinen, K. E. J. and
649 Kerminen, V. M.: Toward direct measurement of atmospheric nucleation, *Science*, 318(5847), 89–92,
650 doi:10.1126/science.1144124, 2007.
- 651 Kulmala, M., Kontkanen, J., Junninen, H., Lehtipalo, K., Manninen, H. E., Nieminen, T., Petäjä, T., Sipilä,
652 M., Schobesberger, S., Rantala, P., Franchin, A., Jokinen, T., Järvinen, E., Äijälä, M., Kangasluoma, J.,
653 Hakala, J., Aalto, P. P., Paasonen, P., Mikkilä, J., Vanhanen, J., Aalto, J., Hakola, H., Makkonen, U.,
654 Ruuskanen, T., Mauldin, R. L., Duplissy, J., Vehkamäki, H., Bäck, J., Kortelainen, A., Riipinen, I., Kurtén,
655 T., Johnston, M. V., Smith, J. N., Ehn, M., Mentel, T. F., Lehtinen, K. E. J. J., Laaksonen, A., Kerminen, V.-
656 M. M. V.-M., Worsnop, D. R., Petaja, T., Sipilä, M., Schobesberger, S., Rantala, P., Franchin, A., Jokinen,
657 T., Jarvinen, E., Aijala, M., Kangasluoma, J., Hakala, J., Aalto, P. P., Paasonen, P., Mikkilä, J., Vanhanen, J.,
658 Aalto, J., Hakola, H., Makkonen, U., Ruuskanen, T., Mauldin, R. L., Duplissy, J., Vehkamäki, H., Back, J.,
659 Kortelainen, A., Riipinen, I., Kurten, T., Johnston, M. V., Smith, J. N., Ehn, M., Mentel, T. F., Lehtinen, K.
660 E. J. J., Laaksonen, A., Kerminen, V.-M. M. V.-M., Worsnop, D. R., Petäjä, T., Sipilä, M., Schobesberger,
661 S., Rantala, P., Franchin, A., Jokinen, T., Järvinen, E., Äijälä, M., Kangasluoma, J., Hakala, J., Aalto, P. P.,
662 Paasonen, P., Mikkilä, J., Vanhanen, J., Aalto, J., Hakola, H., Makkonen, U., Ruuskanen, T., Mauldin, R. L.,
663 Duplissy, J., Vehkamäki, H., Bäck, J., Kortelainen, A., Riipinen, I., Kurtén, T., Johnston, M. V., Smith, J. N.,
664 et al.: Direct observations of atmospheric aerosol nucleation., *Science*, 339(6122), 943–6,
665 doi:10.1126/science.1227385, 2013.
- 666 Kulmala, M., Ezhova, E., Kalliokoski, T., Noe, S., Vesala, T., Lohila, A., Liski, J., Makkonen, R., Bäck, J.,
667 Petäjä, T. and Kerminen, V.-M.: CarbonSink+-Accounting for multiple climate feedbacks from forests,
668 2020.



- 669 Kürten, A., Rondo, L., Ehrhart, S. and Curtius, J.: Calibration of a chemical ionization mass spectrometer for
670 the measurement of gaseous sulfuric acid, *J. Phys. Chem. A*, 116(24), 6375–6386, doi:10.1021/jp212123n,
671 2012.
- 672 Kürten, A., Jokinen, T., Simon, M., Sipilä, M., Sarnela, N., Junninen, H., Adamov, A., Almeida, J., Amorim,
673 A., Bianchi, F., Breitenlechner, M., Dommen, J., Donahue, N. M., Duplissy, J., Ehrhart, S., Flagan, R. C.,
674 Franchin, A., Hakala, J., Hansel, A., Heinritzi, M., Hutterli, M., Kangasluoma, J., Kirkby, J., Laaksonen, A.,
675 Lehtipalo, K., Leiminger, M., Makhmutov, V., Mathot, S., Onnela, A., Petäjä, T., Praplan, A. P., Riccobono,
676 F., Rissanen, M. P., Rondo, L., Schobesberger, S., Seinfeld, J. H., Steiner, G., Tomé, A., Tröstl, J., Winkler,
677 P. M., Williamson, C., Wimmer, D., Ye, P., Baltensperger, U., Carslaw, K. S., Kulmala, M., Worsnop, D. R.,
678 Curtius, J. and Barbara Finlayson-Pitts, by J.: Neutral molecular cluster formation of sulfuric acid–
679 dimethylamine observed in real time under atmospheric conditions, *Proc. Natl. Acad. Sci. U.S.A.*, 111(42),
680 15019–15024, doi:10.1073/pnas.1404853111, 2014.
- 681 Kyrö, E. M., Väänänen, R., Kerminen, V. M., Virkkula, A., Petäjä, T., Asmi, A., Dal Maso, M., Nieminen,
682 T., Juhola, S., Shcherbinin, A., Riipinen, I., Lehtipalo, K., Keronen, P., Aalto, P. P., Hari, P. and Kulmala,
683 M.: Trends in new particle formation in eastern Lapland, Finland: Effect of decreasing sulfur emissions from
684 Kola Peninsula, *Atmos. Chem. Phys.*, 14(9), 4383–4396, 2014.
- 685 Lai, S. C., Williams, J., Arnold, S. R., Atlas, E. L., Gebhardt, S. and Hoffmann, T.: Iodine containing species
686 in the remote marine boundary layer: A link to oceanic phytoplankton, *Geophys. Res. Lett.*, 38(20),
687 doi:10.1029/2011GL049035, 2011.
- 688 Lehtipalo, K., Yan, C., Dada, L., Bianchi, F., Xiao, M., Wagner, R., Stolzenburg, D., Ahonen, L. R.,
689 Amorim, A., Baccarini, A., Bauer, P. S., Baumgartner, B., Bergen, A., Bernhammer, A.-K., Breitenlechner,
690 M., Brilke, S., Buchholz, A., Mazon, S. B., Chen, D., Chen, X., Dias, A., Dommen, J., Draper, D. C.,
691 Duplissy, J., Ehn, M., Finkenzeller, H., Fischer, L., Frege, C., Fuchs, C., Garmash, O., Gordon, H., Hakala,
692 J., He, X., Heikkinen, L., Heinritzi, M., Helm, J. C., Hofbauer, V., Hoyle, C. R., Jokinen, T., Kangasluoma,
693 J., Kerminen, V.-M., Kim, C., Kirkby, J., Kontkanen, J., Kürten, A., Lawler, M. J., Mai, H., Mathot, S.,
694 Mauldin, R. L., Molteni, U., Nichman, L., Nie, W., Nieminen, T., Ojdanic, A., Onnela, A., Passananti, M.,
695 Petäjä, T., Piel, F., Pospisilova, V., Quéléver, L. L. J., Rissanen, M. P., Rose, C., Sarnela, N., Schallhart, S.,
696 Schuchmann, S., Sengupta, K., Simon, M., Sipilä, M., Tauber, C., Tomé, A., Tröstl, J., Väisänen, O., Vogel,
697 A. L., Volkamer, R., Wagner, A. C., Wang, M., Weitz, L., Wimmer, D., Ye, P., Ylisirniö, A., Zha, Q.,
698 Carslaw, K. S., Curtius, J., Donahue, N. M., Flagan, R. C., Hansel, A., Riipinen, I., Virtanen, A., Winkler, P.
699 M., Baltensperger, U., Kulmala, M. and Worsnop, D. R.: Multicomponent new particle formation from
700 sulfuric acid, ammonia, and biogenic vapors, *Sci. Adv.*, 4(12), eaau5363–eaau5363,
701 doi:10.1126/sciadv.aau5363, 2018.
- 702 Leino, K., Nieminen, T., Manninen, H. E., Petäjä, T., Kerminen, V.-M. and Kulmala, M.: Intermediate ions
703 as a strong indicator of new particle formation bursts in a boreal forest, 2016.
- 704 Levasseur, M.: Impact of Arctic meltdown on the microbial cycling of sulphur, *Nat. Geosci.*, 6(9), 691–700,
705 doi:10.1038/ngeo1910, 2013.
- 706 Mäkelä, J. M., Aalto, P., Jokinen, V., Pohja, T., Nissinen, A., Palmroth, S., Markkanen, T., Seitsonen, K.,
707 Lihavainen, H. and Kulmala, M.: Observations of ultrafine aerosol particle formation and growth in boreal
708 forest, *Geophys. Res. Lett.*, 24(10), 1219–1222, doi:10.1029/97GL00920, 1997.
- 709 Manninen, H. E., Mirme, S., Mirme, A., Petäjä, T., and Kulmala, M.: How to reliably detect molecular
710 clusters and nucleation mode particles with Neutral cluster and Air Ion Spectrometer (NAIS), *Atmos. Meas.*
711 *Tech.*, 9, 3577–3605, <https://doi.org/10.5194/amt-9-3577-2016>, 2016.
- 712 McFiggans, G., Bale, C. S. E. E., Ball, S. M., Beames, J. M., Bloss, W. J., Carpenter, L. J., Dorsey, J., Dunk,
713 R., Flynn, M. J., Furneaux, K. L., Gallagher, M. W., Heard, D. E., Hollingsworth, A. M., Hornsby, K.,
714 Ingham, T., Jones, C. E., Jones, R. L., Kramer, L. J., Langridge, J. M., Leblanc, C., LeCrane, J. P.-P., Lee, J.
715 D., Leigh, R. J., Longley, I., Mahajan, A. S., Monks, P. S., Oetjen, H., Orr-Ewing, a. J., Plane, J. M. C. C.,
716 Potin, P., Shillings, a. J. L. L., Thomas, F., Von Glasow, R., Wada, R., Whalley, L. K. and Whitehead, J. D.:
717 Iodine-mediated coastal particle formation: an overview of the Reactive Halogens in the Marine Boundary



- 718 Layer (RH_aMBLe) Roscoff coastal study, *Atmos. Chem. Phys.*, 10(6), 2975–2999, doi:10.5194/acpd-9-
719 26421-2009, 2010.
- 720 Mirme, S. and Mirme, A.: The mathematical principles and design of the NAIS – a spectrometer for the
721 measurement of cluster ion and nanometer aerosol size distributions, *Atmos. Meas. Tech.*, 6(4), 1061–1071,
722 doi:10.5194/amt-6-1061-2013, 2013.
- 723 Myllys, N., Ponkkonen, T., Passananti, M., Elm, J., Vehkamäki, H. and Olenius, T.: Guanidine: A Highly
724 Efficient Stabilizer in Atmospheric New-Particle Formation, *J. Phys. Chem. A*, 122(20), 4717–4729,
725 doi:10.1021/acs.jpca.8b02507, 2018.
- 726 Napari, I., Noppel, M., Vehkamäki, H. and Kulmala, M.: Parametrization of ternary nucleation rates for
727 H₂SO₄-NH₃-H₂O vapors, *J. Geophys. Res. Atmos.*, 107(19), doi:10.1029/2002JD002132, 2002.
- 728 Nieminen, T., Asmi, A., Maso, M. D., Aalto, P. P., Keronen, P., Kulmala, M., Kerminen, V., Dal maso, M.,
729 Aalto, P. P., Keronen, P., Petäjä, T., Kulmala, M. and Kerminen, V.: Trends in atmospheric new-particle
730 formation: 16 years of observations in a boreal-forest environment, *Boreal Environ. Res.*, 19 (suppl.(2004)),
731 191–214, 2014.
- 732 O’Dowd, C. D., Jimenez, J. L., Bahreini, R., Flagan, R. C., Seinfeld, J. H., Hämerl, K., Pirjola, L., Kulmala,
733 M. and Hoffmann, T.: Marine aerosol formation from biogenic iodine emissions, *Nature*, 417(6889), 632–
734 636, 2002.
- 735 Paasonen, P., Asmi, A., Petäjä, T., Kajos, M. K., Äijälä, M., Junninen, H., Holst, T., Abbatt, J. P. D. D.,
736 Arneth, A., Birmili, W., Van Der Gon, H. D., Hamed, A., Hoffer, A., Laakso, L., Laaksonen, A., Richard
737 Leaitch, W., Plass-Dülmer, C., Pryor, S. C., Räisänen, P., Swietlicki, E., Wiedensohler, A., Worsnop, D. R.,
738 Kerminen, V.-M. M. and Kulmala, M.: Warming-induced increase in aerosol number concentration likely to
739 moderate climate change, *Nat. Geosci.*, 6(6), 438–442, doi:10.1038/ngeo1800, 2013.
- 740 Park, K., Lee, K., Kim, T., Yoon, Y. J., Jang, E., Jang, S., Lee, B. and Hermansen, O.: Atmospheric DMS in
741 the Arctic Ocean and Its Relation to Phytoplankton Biomass, *Global Biogeochem. Cycles*, 32(3), 351–359,
742 doi:10.1002/2017GB005805, 2018.
- 743 Pirjola, L., Laaksonen, A., Aalto, P. and Kulmala, M.: Sulfate aerosol formation in the Arctic boundary
744 layer, *J. Geophys. Res. Atmos.*, 103(D7), 8309–8321, doi:10.1029/97JD03079, 1998.
- 745 Raso, A. R. W., Custard, K. D., May, N. W., Tanner, D., Newburn, M. K., Walker, L., Moore, R. J., Huey,
746 L. G., Alexander, L., Shepson, P. B. and Pratt, K. A.: Active molecular iodine photochemistry in the Arctic,
747 *Proc. Natl. Acad. Sci. U. S. A.*, 114(38), 10053–10058, doi:10.1073/pnas.1702803114, 2017.
- 748 Reyer, C. P. O., Brouwers, N., Rammig, A., Brook, B. W., Epila, J., Grant, R. F., Holmgren, M.,
749 Langerwisch, F., Leuzinger, S., Lucht, W., Medlyn, B., Pfeifer, M., Steinkamp, J., Vanderwel, M. C.,
750 Verbeeck, H. and Vilella, D. M.: Forest resilience and tipping points at different spatio-temporal scales:
751 Approaches and challenges, *J. Ecol.*, 103(1), 5–15, doi:10.1111/1365-2745.12337, 2015.
- 752 Riva, M., Rantala, P., Krechmer, E. J., Peräkylä, O., Zhang, Y., Heikkinen, L., Garmash, O., Yan, C.,
753 Kulmala, M., Worsnop, D. and Ehn, M.: Evaluating the performance of five different chemical ionization
754 techniques for detecting gaseous oxygenated organic species, *Atmos. Meas. Tech.*, 12(4), 2403–2421,
755 doi:10.5194/amt-12-2403-2019, 2019.
- 756 Ruuskanen, T., Reissell, M., Keronen, A., Aalto, P. P., Laakso, P. P., Grönholm, L., Hari, T. and Kulmala,
757 P.: Atmospheric trace gas and aerosol particle concentration measurements in Eastern Lapland, *Boreal Env.*
758 *Res.*, 8, 335–349, 2003.
- 759 Ruuskanen, T. M., Kaasik, M., Aalto, P. P., Hörrak, U., Vana, M., Mårtensson, M., Yoon, Y. J., Keronen, P.,
760 Mordas, G., Ceburnis, D., Nilsson, E. D., O’Dowd, C., Noppel, M., Alliksaar, T., Ivask, J., Sofiev, M.,
761 Prank, M. and Kulmala, M.: Concentrations and fluxes of aerosol particles during the LAPBIAT
762 measurement campaign at Värriö field station, *Atmos. Chem. Phys.*, 7(14), 3683–3700, doi:10.5194/acp-7-
763 3683-2007, 2007.



- 764 Schmale, J., Zieger, P. and Ekman, A. M. L.: Aerosols in current and future Arctic climate, *Nat. Clim. Chang.*, 11(2), 95–105, doi:10.1038/s41558-020-00969-5, 2021.
- 766 Seco, R., Holst, T., Sillesen Matzen, M., Westergaard-Nielsen, A., Li, T., Simin, T., Jansen, J., Crill, P.,
767 Friborg, T., Rinne, J. and Rinnan, R.: Volatile organic compound fluxes in a subarctic peatland and lake,
768 *Atmos. Chem. Phys.*, 20(21), 13399–13416, doi:10.5194/ACP-20-13399-2020, 2020.
- 769 Sherwen, T. M., Evans, M. J., Spracklen, D. V., Carpenter, L. J., Chance, R., Baker, A. R., Schmidt, J. A.
770 and Breider, T. J.: Global modeling of tropospheric iodine aerosol, *Geophys. Res. Lett.*, 43(18), 10012–
771 10019, doi:10.1002/2016gl070062, 2016.
- 772 Sipilä, M., Sarnela, N., Jokinen, T., Henschel, H., Junninen, H., Kontkanen, J., Richters, S., Kangasluoma, J.,
773 Franchin, A., Peräkylä, O., Rissanen, M. P., Ehn, M., Vehkamäki, H., Kurten, T., Berndt, T., Petäjä, T.,
774 Worsnop, D., Ceburnis, D., Kerminen, V.-M. M., Kulmala, M., O'Dowd, C. and O'Dowd, C.: Molecular-
775 scale evidence of aerosol particle formation via sequential addition of HIO₃, *Nature*, 537(7621), 532–534,
776 doi:10.1038/nature19314, 2016.
- 777 Sipilä, M., Sarnela, N., Neitola, K., Laitinen, T., Kemppainen, D., Beck, L., Duplissy, E.-M., Kuittinen, S.,
778 Lehmusjärvi, T., Lampilahti, J., Kerminen, V.-M., Lehtipalo, K., Aalto, P., Keronen, P., Siivola, E., Rantala,
779 P., Worsnop, D., Kulmala, M., Jokinen, T. and Petäjä, T.: Wintertime sub-arctic new particle formation from
780 Kola Peninsula sulphur emissions, *Atmos. Chem. Phys. Discuss.*, 1–27, doi:10.5194/acp-2020-1202, 2021.
- 781 Sive, B. C., Varner, R. K., Mao, H., Blake, D. R., Wingenter, O. W. and Talbot, R.: A large terrestrial source
782 of methyl iodide, *Geophys. Res. Lett.*, 34(17), L17808, doi:10.1029/2007gl030528, 2007.
- 783 Spolaor, A., Barbaro, E., Cappelletti, D., Turetta, C., Mazzola, M., Giardi, F., Björkman, M., Lucchetta, F.,
784 Dallo, F., Pfaffhuber, K. A., Angot, H., Dommergue, A., Maturilli, M., Saiz-Lopez, A., Barbante, C. and
785 Cairns, W.: Diurnal cycle of iodine and mercury concentrations in Svalbard surface snow, *Atmos. Chem.*
786 *Phys. Discuss.*, 1–25, doi:10.5194/ACP-2019-285, 2019.
- 787 Stohl, A.: Characteristics of atmospheric transport into the Arctic troposphere, *J. Geophys. Res. Atmos.*, 111,
788 D11306, doi:10.1029/2005JD006888, 2006.
- 789 Sulo, J., Sarnela, N., Kontkanen, J., Ahonen, L., Paasonen, P., Laurila, T., Jokinen, T., Kangasluoma, J.,
790 Junninen, H., Sipilä, M., Petäjä, T., Kulmala, M. and Lehtipalo, K.: Long-term measurement of sub-
791 3 nm particles and their precursor gases in the boreal forest, *Atmos. Chem. Phys.*, 21(2), 695–715,
792 doi:10.5194/acp-21-695-2021, 2021.
- 793 Tarvainen, V., Hakola, H., Hellén, H., Bäck, J., Hari, P. and Kulmala, M.: Temperature and light dependence
794 of the VOC emissions of Scots pine, *Atmos. Chem. Phys. Discuss.*, 4(5), 6691–6718, doi:10.5194/acpd-4-
795 6691-2004, 2004.
- 796 Tiiva, P., Faubert, P., Michelsen, A., Holopainen, T., Holopainen, J. K. and Rinnan, R.: Climatic warming
797 increases isoprene emission from a subarctic heath, *New Phytol.*, 180(4), 853–863, doi:10.1111/J.1469-
798 8137.2008.02587.X, 2008.
- 799 Tunved, P., Hansson, H. C., Kerminen, V. M., Ström, J., Dal Maso, M., Lihavainen, H., Viisanen, Y., Aalto,
800 P. P., Komppula, M. and Kulmala, M.: High natural aerosol loading over boreal forests, *Science*, 312(5771),
801 261–263, doi:10.1126/science.1123052, 2006.
- 802 Valolahti, H., Kivimäenpää, M., Faubert, P., Michelsen, A. and Rinnan, R.: Climate change-induced
803 vegetation change as a driver of increased subarctic biogenic volatile organic compound emissions, *Glob.*
804 *Chang. Biol.*, 21(9), 3478–3488, doi:10.1111/GCB.12953, 2015.
- 805 Vana, M., Komsaare, K., Hörrak, U., Mirme, S., Nieminen, T., Kontkanen, J., Manninen, H. E., Petäjä, T.,
806 Noe, S. M. and Kulmala, M.: Characteristics of new-particle formation at three SMEAR stations, *Boreal.*
807 *Env. Res.* 21: 345–362, 2016.
- 808 Vehkamäki, H., Dal Maso, M., Hussein, T., Flanagan, R., Hyvärinen, A., Lauros, J., Merikanto, J.,
809 Mönkkönen, P., Pihlatie, M., Salminen, K., Sogacheva, L., Thum, T., Ruuskanen, T. M., Keronen, P., Aalto,



- 810 P. P., Hari, P., Lehtinen, K. E. J., Rannik, Ü. and Kulmala, M.: Atmospheric particle formation events at
811 Värriö measurement station in Finnish Lapland 1998-2002, *Atmos. Chem. Phys.*, 4(7), 2015–2023,
812 doi:10.5194/acp-4-2015-2004, 2004.
- 813 Wang, S., Riva, M., Yan, C., Ehn, M. and Wang, L.: Primary Formation of Highly Oxidized Multifunctional
814 Products in the OH-Initiated Oxidation of Isoprene: A Combined Theoretical and Experimental Study,
815 *Environ. Sci. Technol.*, 52(21), 12255–12264, doi:10.1021/acs.est.8b02783, 2018.
- 816 Wang, Y. Q., Zhang, X. Y. and Draxler, R. R.: TrajStat: GIS-based software that uses various trajectory
817 statistical analysis methods to identify potential sources from long-term air pollution measurement data,
818 *Environ. Model. Softw.*, 24(8), 938–939, doi:10.1016/j.envsoft.2009.01.004, 2009.
- 819 Yu, H., Ren, L., Huang, X., Xie, M., He, J. and Xiao, H.: Iodine speciation and size distribution in ambient
820 aerosols at a coastal new particle formation hotspot in China, *Atmos. Chem. Phys.*, 19(6), 4025–4039,
821 doi:10.5194/acp-19-4025-2019, 2019.
- 822